

Mineralogical Characterization of Weathered Outcrops as a Tool for Constraining Water Chemistry Predictions during Project Planning

Tamara Diedrich¹, Paul Fix², and Andrea Foster³

¹*MineraLogic LLC, Duluth, MN; tdiedrich@mineralogicllc.com*

²*Univeristy of Minnesota Duluth; Duluth, MN*

³*U.S. Geological Survey, Menlo Park, CA; afoster@usgs.gov*

Abstract Weathered samples from naturally exposed outcrops of troctolite associated with a magmatic Ni-Cu sulphide deposit were characterized by synchrotron-based micro-X-ray fluorescence mapping (μ -XRF) and X-ray absorption spectroscopy (XAS), as well as by lab-based X-ray diffraction, electron microscopy, Raman spectroscopy and wet chemical methods. Metal mobility in weathered samples was assessed using a sequential leach procedure. Results are interpreted in the context of predictions for future mine water chemistry and used to refine the conceptual model for metal mobility following weathering of waste rock at a potential future mine site.

Key words spectroscopy, XAS, XRF, EPMA, XRD, Raman, copper, weathering, alteration

Introduction

Water chemistry predictions used for mine planning and environmental review tend to rely heavily on geochemical characterization of relatively “fresh” rock samples. While these samples may represent the condition of geologic materials as they will be excavated and initially managed during mining operations, they do not capture the evolution in mineral surfaces and formation of weathering products that occur as rock is exposed to surficial conditions over longer timescales. These weathering products attenuate dissolved metals through sorption or (co-)precipitation of secondary phases, and may release these stored metals should conditions change (for example, relocation to a subaqueous environment). Therefore, realistic prediction of mine impacted water chemistry at operational scales requires conceptual and geochemical models in which the weathering products and key reactions have been accurately identified.

This paper reports the characterization of weathering products associated with low sulphide outcrops of a magmatic copper (Cu) – nickel (Ni) sulphide deposit and the application of that characterization data as a tool for constraining pre-operational predictions of water chemistry. In this preliminary report, we characterize Cu-bearing, Fe (hydr)oxide weathering products at the micron scale, and use this information, along with results on copper release from sequential leach tests, to refine a conceptual model for the release and potential mobility of copper following weathering of non-ore grade rock.

Geologic Context

Samples characterized for this study were collected from outcrops of the Duluth Complex, a large composite mafic intrusion located in northeastern Minnesota, USA. Basal portions

of the complex contain copper-nickel-PGE magmatic sulphide deposits, hosted largely by troctolitic rocks (plagioclase + olivine +/- pyroxene; Miller et al. 2002; Severson and Hauck 2008). Multiple deposits in the Duluth Complex are currently being developed as potential future copper-nickel-PGE mines. Sulphide mineralization consists of pyrrhotite, chalcopyrite, cubanite and pentlandite, generally occurring as disseminated grains among silicate phases in the troctolite, but also as veinlets, inclusions in silicates, intergrowths with hydrous minerals, and as rare massive sulphide segregations (Miller et al. 2002).

The geochemistry of Duluth Complex waste rock has been well studied by project proponents and by the research program at the Minnesota Department of Natural Resources. Sulphate, acidity, and metals are released through the oxidation of sulphide minerals, primarily pyrrhotite. The rock does not contain appreciable carbonate minerals; neutralization potential is provided by dissolution of abundant calcium-rich plagioclase and olivine. Due to the geometry of mineralization within the Duluth Complex (located along the base of intrusions) deposits are associated with significant quantities of low sulphide, non-potentially acid generating, non-ore grade rock. However, even in the absence of acidic drainage, there is some potential for elevated concentrations of dissolved metals in contact water. Therefore, identifying the factors that control the mobility of metals is relevant to development of Duluth Complex projects.

Methods

Six samples from five visibly weathered outcrops at the site of a potential future copper-nickel mine of a Duluth Complex deposit were sampled with the intent of capturing a representative range of weathering products. Samples were collected as grab samples consisting of small clasts and rubble (typically less than 1 to 2 inches), and also larger (several inches in diameter) intact hand samples. The techniques used to characterize the mineralogy and chemistry of weathering products are described briefly below.

Thin section preparation. Samples were impregnated with low-trace element, low-temperature curing epoxy (EPOTEK-301-2FL), bonded to quartz slides. then cut and polished (under oil) to the standard 30 micron-thickness of petrographic sections.

X-ray Diffraction. Crystalline weathering products were identified in bulk material with a Phillips XPert MPD diffractometer at the University of Minnesota Duluth (USA) with a Cu K α radiation source. Each sample was scanned between 5° and 65° 2 θ at a scan rate of 0.05 deg. /min. Long collection times (~15 hrs.) were used to increase signal to noise ratios. Diffraction data were processed with X-Pert HighScore software and compared to mineral patterns in the International Centre for Diffraction Data database (ICDD 2007).

Sequential Leach. Grab samples were crushed, homogenized, and split into subsamples. One subsample from each was subjected to standard acid base accounting procedures, including analysis of the total sulphur content by LECO furnace combustion. Another subsample was subjected to six sequential extraction steps: particular focus in this paper is

given to the amount of Cu released in the “oxidizable” and “reducible” steps [as defined by Chao and Zhou (1983) and Leinz and Sutley (2000), respectively].

Scanning Electron Microscopy/Electron Microprobe. Images of average backscatter electron intensity [e.g., fig. 1a] were collected using standard scanning electron microscopes at U. Minnesota, Duluth, and the USGS in Menlo Park, CA, USA. Micron-scale compositional data were obtained on a JEOL JXA-8800L Superprobe at the USGS-Menlo Park from carbon-coated thin sections. The instrument was operated at 15 kV and 15 nA with an approximate incident beam spot of 1 mm diameter. Standard CITZAF corrections were applied to the data, which is expressed as weight % oxide, or as element %. Under these conditions, the detection limit for Cu was approximately 0.025 atom % (250 mg/kg), and the standard deviation of analyzed values was ~12%.

Raman Spectroscopy. Micro-Raman spectra were collected from uncoated thin sections using a Thermo Fisher DXR system at the USGS, Menlo Park, CA, USA. The system was equipped with a 532 nm laser, 50 cm⁻¹ Rayleigh rejection filter, a grating with 900 lines per mm, and a Peltier-cooled 2048 pixel CCD detector. The collected spectra spanned the range 50-3399 cm⁻¹ (3475 total points) with resolution of ± 5 cm⁻¹.

Synchrotron μ-XRF/XAS. Micron-scale information on element distribution and copper speciation was obtained from coated or uncoated thin sections via μ-XRF mapping and XAS data collected at the Stanford Synchrotron Radiation Lightsource (Menlo Park, CA, USA; beamline II-3). The focusing optics produce a pseudo circular beam of ≈ 2 micron diameter. Beam energy was calibrated at 8984 eV using elemental Cu foil. The Cu Kα X-ray map shown in fig. 1b was produced by moving the sample over a region of interest in 2 micron steps with a dwell time of 50 milliseconds per step. X-ray maps were processed and analyzed using MicroToolkit (version 1.1-1.2; Webb 2005).

X-ray absorption spectra at the Cu K-edge were collected from points of interest identified from μ-XRF maps. Spectra were collected over the energy range 8809-9365 eV, with appropriate count time and step size for the background, edge, and extended regions of the XAS spectrum (1 sec/10 eV, 1 sec/0.35 eV, and 2-5 sec/0.6-4 eV, respectively). Spectra were processed and analysed in the program SixPack (versions 1.2-1.4; Webb 2005). XAS spectra were fit over the energy range 8960-9160 eV using the “cycle fit” linear-combination, least-squares approach that minimizes overfitting of the data and has estimated error and detection limit of about 10% each (Kim et al. 2014).

Results and Discussion

Mineralogy of Fe(hydr)oxide bands. Characterization of weathering products via X-ray diffraction indicated the presence of the minerals rozenite, malachite, and goethite. Patterns from several samples displayed very broad peaks, roughly corresponding to peak positions of goethite and/or ferrihydrite, consistent with an interpretation that these products are amorphous to poorly-crystalline hydrous iron oxide minerals. This conclusion was supported by MicroRaman spectroscopy, in which most spectra of banded Fe-hydroxide

contained the two most intense Raman bands for goethite (386 cm^{-1} and 300 cm^{-1} , respectively; Cornell and Schwertmann 2003) but far fewer contained even 5 of the 9 bands observable in a reference spectrum of highly crystalline goethite (RUFF ID R050142; Lafuente et al. 2015).

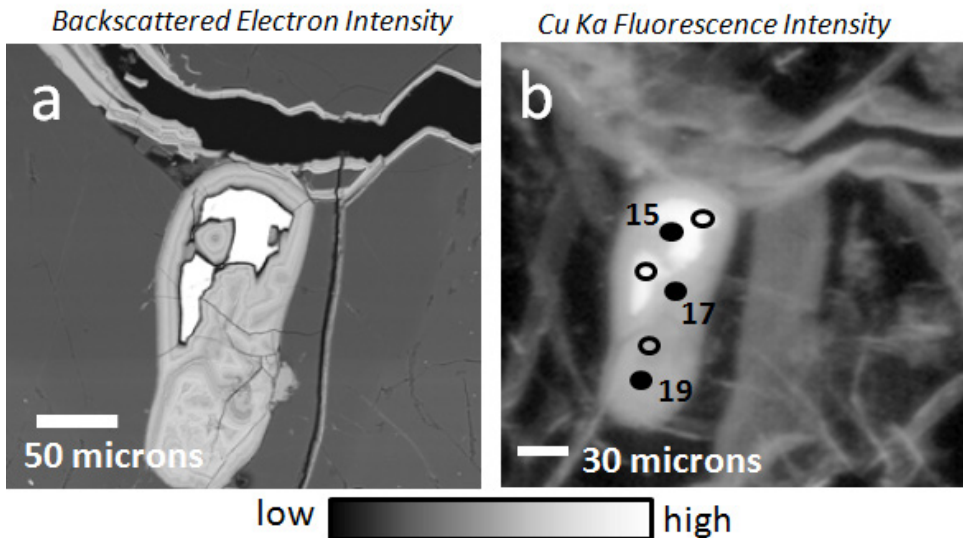


Figure 1 (a) SEM micrograph of weathered Duluth Complex sample containing relic chalcopyrite (brightest areas) replaced by banded Fe(hydr)oxide, and banded Fe hydroxide lining a large fracture. (b) u-XRF map Cu Ka intensity, revealing Cu-rich regions (at depth in the 30 mm section) not apparent from the BSE image.

Chemistry of Fe(hydr)oxide bands. Alternating light/dark bands, each about 2-20 microns thick, are visible in backscattered electron images of weathering rinds replacing chalcopyrite grains and in fracture fill (Fig. 1a). The banding is primarily due to differences in the relative abundance of Fe and Si; Fe (as FeO) is higher in light bands than in dark ones (54.1 wt% and 46.9 wt%, respectively), whereas Si (as SiO_2) shows the reverse trend (16.1 wt% and 22.0 wt%, respectively; median values of 8 determinations for all).

Additionally, two distinct compositional populations of this Si-rich, Cu-bearing Fe (hydr) oxide are observed: a “high Cu” form that replaces chalcopyrite and a “low Cu” form that fills fractures, often at considerable distance from relic sulfide grains. The “high Cu” Fe(hydr) oxide contains 7.1 wt% and 2.9 wt% CuO in light and dark bands, respectively, for a difference of about 4.2% CuO between light and dark bands. The “low Cu” Fe(hydr)oxide has a much smaller difference (0.2 wt %) between the average Cu content of light and dark bands (which is 2.3% CuO, approximately the same Cu concentration as in the BSE-dark bands of “high Cu” Fe hydroxide.).

Copper speciation in Fe (hydr)oxide bands. X-ray absorption near-edge spectroscopy (XANES) in the Cu near-edge region is sensitive to the molecular configuration of Cu as

well as to its valence state. The spectra in fig. 2a are all from samples in which Cu adopts an octahedral coordination, but subtle differences in shape, width, and position of peaks can be observed.

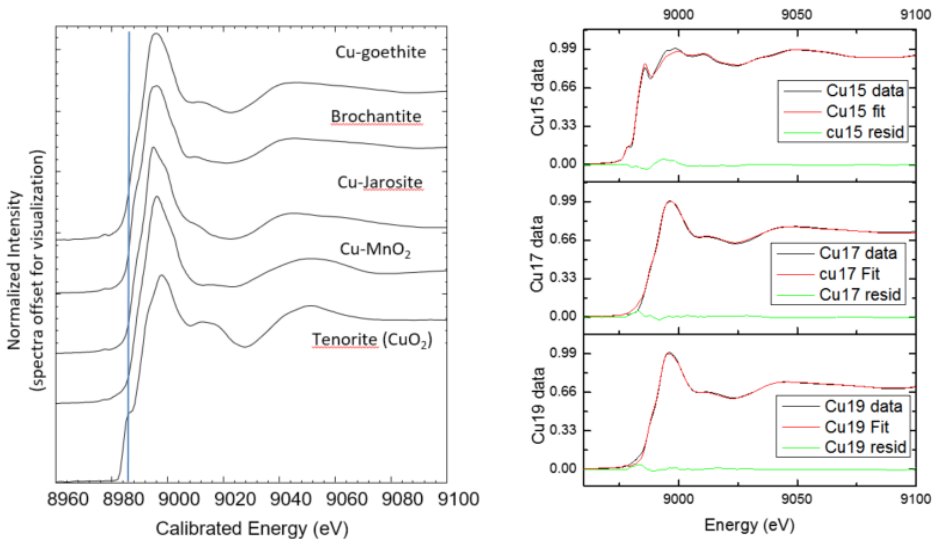


Figure 2 (a) stack plot of Cu-K edge XANES spectra of Cu model compounds with Cu in 6-fold coordination by oxygen atoms/hydroxyl groups. Copper was either sorbed (goethite, MnO₂) or (co)-precipitated (brochantite, jarosite). The tenorite spectrum was taken from a database of XAS spectra. (b) Results of linear-combination, least-squares fits to XANES spectra collected from points shown in Figure 1b.

Linear combination, least-squares fits to representative Cu K-edge XANES spectra are shown in fig. 2b (see fig. 1b for analyzed locations). The topmost panel shows the spectrum, fit, and fit residual of spot 15, just at the edge of a chalcopyrite grain. Using a model spectrum of chalcopyrite alone provided a good fit. The bottom 2 panels show data and fits from spots located close to and more distal from intact chalcopyrite (17 and 19, respectively). The spectra from these spots were fit best by approximately 80% Cu adsorbed to goethite (Kimball et al. 2016). The spectrum of Cu adsorbed to goethite could also represent Cu coprecipitated in goethite, based on analogy to other systems (e.g., Waychunas et al. 1993). The identity of the lower-abundance Cu species could not be determined with certainty; fits of equal statistical quality were obtained when any of the other models in fig. 2a were used (with the exception of tenorite, which was rejected in fits).

While this study does not distinguish between Cu adsorbed to versus coprecipitated in goethite on the basis of the XANES spectra, a previous study concluded that Cu coprecipitates in goethite resulting from peridotite weathering on the basis of detailed fits to natural samples and co-precipitates with goethite synthesized in the laboratory (Manceau et al. 2000).

Sequential leach tests. All samples contained significant copper in both the reducible and oxidizable fractions of the 6-step leach. Assuming that the reducible fraction is solely attributed to Fe (hydr)oxide, its calculated copper content would range between 1–3%, which is consistent with the observed concentrations of copper in the “low Cu” Fe(hydr)oxide fracture fillings and in the darker Fe(hydr)oxide bands around chalcopyrite.

Assuming that the oxidizable fraction can be attributed solely to sulphide minerals, the calculated copper content of the sulphide mineral fraction (copper tenor) is between 20–40%. These values range above the copper content of chalcopyrite (34.6%), and are over twice as high as published copper tenor for ores from related deposits (17%; Naldrett 2004). Additionally, the oxidizable iron to sulfide sulfur ratio reaches in excesses of 20:1, far greater than that of a sulfide mineral. Thus, the apparent excess of copper and iron reporting to the oxidizable fraction would be consistent with some fraction of the Fe(hydr)oxide persisting through the reducing leach step. This could be due to protective “armoring” of the Fe(hydroxide) by the silica-rich layers, or it could be due to an incomplete reaction of the reductant with partially-crystalline phases.

Table 1 Selected results of the sequential leaching procedure with calculated copper contents of the iron oxide bands and sulphide mineral fraction.

Sample	[S] (%) ¹	[Cu] (%)		[Fe] (%)	[CuO] of Fe _{ox} (%) ²	[Cu] of Sulphide Mineral Fraction (%) ³
		Reducible	Oxidizable			
M-SM 001	0.06	0.13	0.07	4.1/2.0	3%	40%
M-SM 002	0.14	0.07	0.13	5.2/2.8	1%	32%
M-SM 004	0.23	0.18	0.23	5.0/2.3	3%	35%
M-SM 004b	0.66	0.11	0.53	4.6/3.6	2%	28%
M-SM 005	0.87	0.08	0.51	3.6/3.9	2%	20%
M-SM 006	0.46	0.09	0.34	5.1/4.1	1%	26%

¹Sulfur as sulfide mineral, determined by combustions via LECO analysis, with and without a HCl leach.

²Calculated assuming that the reducible fraction of Cu or Fe is attributed to Fe (hydr)oxides.

³Calculated assuming that the oxidizable fraction can be attributed to sulphide minerals.

Conclusions: Conceptual model and its implications for Cu mobility during weathering and storage of mine wastes

Mineralogic, chemical, and spectroscopic evidence presented here suggests that a portion of the copper released during oxidation of chalcopyrite in Duluth Complex rock is retained in Fe (hydr)oxide rims that form directly around (and replace) chalcopyrite and in more distal locations as fracture fill. Both types of banded Fe(hydr)oxide are composed primarily of Si-rich, poorly crystalline goethite, with an overall average Cu concentration of about 3% (as CuO).

The most probable conceptual model for Cu speciation in Fe (hydr)oxide based on our data

is on in which Cu occurs predominantly as a co-precipitate rather than adsorbed species, and, therefore, predictive models of copper concentration in mine contact water should include terms to reflect the coprecipitation of copper with goethite. This distinction could have significant implications for water quality, based on experimental leach tests indicating that up to one order of magnitude less Cu is released from a Cu-Fe (hydr)oxide coprecipitate than from a Cu-Fe (hydr)oxide adsorption sample or even from Cu(OH)₂ (pH range: 6-9; Karthikeyan et al. 1997).

Resistance of the Fe (hydr)oxide bands to the reducing leach step implies that these bands may be effective at sequestering Cu even if relocated to an environment depleted in oxygen, such as conditions typical of subaqueous disposal. However, the degree and time scales over which this attenuation could be expected to last would require further evaluation.

Acknowledgements

We gratefully acknowledge the support of Teck American Incorporated, insights and work of Steve Day and Chris Kennedy, and well as, Bronwen Forsyth, of SRK, who designed and oversaw the sequential leach test procedure. Use of the Stanford Synchrotron Radiation Lightsource, SLAC National Accelerator Laboratory, is supported by the U.S. Department of Energy, Office of Science, Office of Basic Energy Sciences under Contract No. DE-AC02-76SF00515. This research was conducted under SSRL proposal #4337.

References

- Chao, TT, Zhou L (1983) Extraction techniques for selective dissolution of amorphous iron oxides from soils and sediments. *Soil Sci Soc Am J* 47:225–232.
- Karthikeyan KG, Elliott HA, Cannon FS (1997) Adsorption and coprecipitation of copper with the hydrous oxides of iron and aluminum. *Environ Sci Technol* 31:2721–2725. doi: 10.1021/es9609009.
- Kim CS, Chi C, Miller SR, Rosales RA, Sugihara ES, Akau J, Rytuba JJ, Webb SM (2013) (Micro) spectroscopic analyses of particle size dependence on arsenic distribution and speciation in mine wastes. *Environ Sci Technol* 47: 8164–8171. doi: 10.1021/es4010653.
- Kimball BE, Foster AL, Seal RR, Piatak NM, Webb SM, Hammarstrom, JM (2016) Copper Speciation in Variably Toxic Sediments at the Ely Copper Mine, Vermont, United States. *Environ Sci Technol* 50: 1126–1136. doi: 10.1021/acs.est.5b04081.
- Lafuente B, Downs RT, Yang H, Stone N (2015) The power of databases: the RRUFF project, in: Danisi, T.A.a.R.M. (Ed.), *Highlights in Mineralogical Crystallography*. W. De Gruyter, Berlin, Germany, pp. 1–30.
- Leinz RW, Sutley SJ (2000) An investigation of the partitioning of metals in mine wastes using sequential extractions. *5th Int Conf Acid Rock Drain* 1–11.
- Manceau A, Schlegel M, Musso M (2000) Crystal chemistry of trace elements in natural and synthetic goethite. *Geochim Cosmochim Acta* 64:3643–3661. doi: 10.1016/S0016-7037(00)00427-0.
- Miller JD, Jr, Green JC, Severson MJ, Chandler VW, Hauck SA, Peterson DM, Wahl TE (2002) Geology and mineral potential of the Duluth Complex and related rocks of northeastern Minnesota: Minnesota Geological Survey Report of Investigations 58. p 207.
- Naldrett AJ (2004) *Magmatic sulfide deposits: geology, geochemistry and exploration*. Springer Science & Business Media.
- Schwertmann, U, Cornell RM (2003) *The Iron Oxides: Structure, Properties, Reactions, Occurrences and Uses*, Second Edition. Wiley-VCH GmbH & Co. KGaA, Weinheim.

- Severson, MJ, Hauck SA (2008) Finish Logging of Duluth Complex Drill Core (And a Reinterpretation of the Geology at the Mesaba (Babbitt) Deposit): University of Minnesota Duluth, Natural Resources Research Institute, Technical Report NRRI/TR-2008/17. Waychunas GA, Rea BA, Fuller CC, Davis JA (1993) Surface chemistry of ferrihydrite: part1. EXAFS studies of the geometry of coprecipitated and adsorbed arsenate. *Geochim Cosmochim Acta* 57: 2251-2269.
- Webb SM (2005) Sixpack: A graphical user interface for XAS analysis using IFEFFIT. *Physica Scripta*, T1115: 1011-1014.
- Webb SM (2005) The MicroAnalysis Toolkit: X-ray Fluorescence Image Processing Software. AIP Conference Proceedings: 196-199.
- International Centre for Diffraction Data (ICDD), 2007.